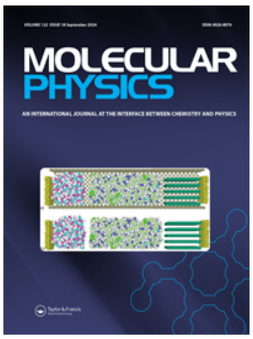

Taylor & Francis
Taylor & Francis Group

Molecular Physics

An International Journal at the Interface Between Chemistry and Physics

ISSN: (Print) (Online) Journal homepage: www.tandfonline.com/journals/tmph20

Impact of sulfate salts on water structure: insights from molecular dynamics

Cintia P. Lamas, Carlos Vega & Paola Gallo

To cite this article: Cintia P. Lamas, Carlos Vega & Paola Gallo (27 Sep 2024): Impact of sulfate salts on water structure: insights from molecular dynamics, Molecular Physics, DOI: 10.1080/00268976.2024.2406260

To link to this article: https://doi.org/10.1080/00268976.2024.2406260

MOLECULAR PHYSICS e2406260
https://doi.org/10.1080/00268976.2024.2406260

Taylor & Francis
Taylor & Francis Group

RULL-ABASCAL SPECIAL ISSUE FOR STATISTICAL PHYSICS IN SPAIN (BY INVITATION ONLY)

Impact of sulfate salts on water structure: insights from molecular dynamics

Cintia P. Lamas [a], Carlos Vega [a] and Paola Gallo [b]

[a]Departamento de Química-Física I (Unidad de I+D+i asociada al CSIC), Facultad de Ciencias Químicas, Universidad Complutense de Madrid, Madrid, Spain; [b]Dipartimento di Matematica e Fisica, Universitá Roma Tre, Roma, Italy

ABSTRACT

Ions significantly alter the water's structure, impacting properties such as the temperature of maximum density and the freezing point. We study structural changes in water upon adding sulfate anions, specifically Na_2SO_4, K_2SO_4, Li_2SO_4, and $MgSO_4$, using computer simulations. We employ the TIP4P/2005 water and the Madrid-2019 force field. By simulating solutions at various concentrations (0.64, 1.30, 1.90, and 3 mol kg^{-1}) and two temperatures (300 and 240 K), we explore how these electrolytes disrupt water's structure and how they modify the interplay between Low Density Water and High Density Water. Increased salt concentration perturbed water's radial distribution functions (RDFs), particularly up to 240 K. Na_2SO_4 significantly disrupted water structure, reducing RDF peak heights and indicating decreased tetrahedrality, while $MgSO_4$ increased structural order. K_2SO_4 displayed anomalous behaviour, minimally affecting water at 1.90 mol kg^{-1} and ambient temperature but causing more ordered structures at 240 K. Orientational order parameter q_t analysis supported these findings. Hydrogen bond network analysis showed notable perturbations at lower temperatures. Diffusion coefficients generally decreased with concentration, with K_2SO_4 exhibiting increase at 240 K. These results highlight the complex interactions between sulfate ions and water, enhancing our understanding of electrolyte solutions.

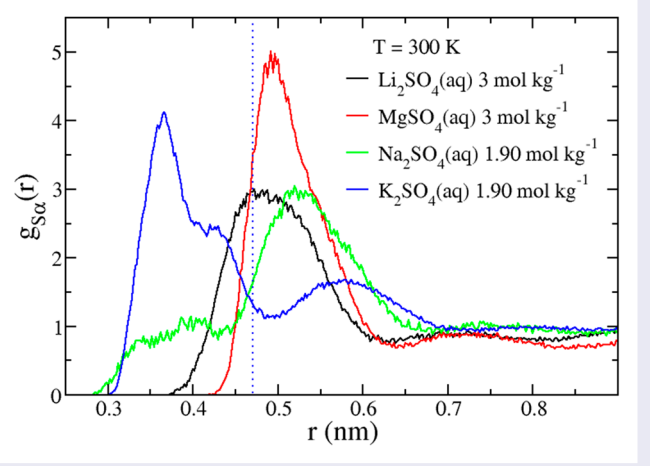

ARTICLE HISTORY
Received 26 July 2024
Accepted 10 September 2024

KEYWORDS
Sulfate aqueous solutions; structure of water; molecular dynamics; Madrid-2019 force field

1. Introduction

When an ionic salt is added to water, it dissociates into ions, and these ions modify the structure of water. The impact of the change is different for different ions, which can be attributed to differences in size, charge (including the sign), and shape (in the case of polyatomic ions [1]). The properties of water change significantly when an electrolyte is dissolved.

When studying aqueous solutions we must take in consideration that water is a special liquid that displays many anomalies that enhance upon supercooling [2]. The interest in understanding the peculiar behaviour of water at low temperatures has been present in the last three decades. The interplay between a High Density Liquid (HDL) and a Low Density Liquid (LDL) structure is connected to this peculiar behaviour [3,4]. In the

CONTACT Paola Gallo paola.gallo@uniroma3.it Dipartimento di Matematica e Fisica, Universitá Roma Tre, Via della Vasca Navale 84, Roma 00146, Italy

supercooled region the existence of these two structures implies the possible existence of a second liquid-liquid critical point [5].

Since ions significantly modify the properties of water, it seems of interest to study in detail the structural changes that occur at low temperatures. A key anomaly of pure water is the presence of a line of maximum in density in the phase diagram. At ambient pressure the density maximum occurs in pure water at about 4 degrees Celsius. For temperatures below this maximum, the density of water decreases when cooling due to the prevalence of more open (LDL) structures induced by the hydrogen bonding network. Above this temperature, the density decreases (as in a normal liquid).

When a salt is added to water, up to a certain concentration, the density maximum is moved to lower temperatures. For instance experiments showed that for a 1 mol kg^{-1} solution (i.e. one mole of salt per kg of water), the maximum is shifted by 5–20 degrees, depending on the salt [6]. This significant effect indicates that the ions indeed disrupt the structure of water. Notice that for a 1 mol kg^{-1} solution, there are about 28 molecules of water per ion for a 1:1 electrolyte, so even a four percent population of ions provokes important changes. Experimental studies (using, for instance, X-ray or neutron diffraction) can certainly help in analysing the changes provoked in the structure of water due to the ions [6–15]. However, these studies face a difficulty: the structure factor is unique, and there are about 10 radial distribution functions (RDF) to be determined even for a system as simple as NaCl in water.

Computer molecular simulation is a valuable tool for its ability to access the nanoscopic scale. As a result, various simulation studies have explored different aspects of salt solutions [16–38].

In this context, computer simulations can certainly help in analysing the structural changes provoked by the presence of salt in water [35,39–42]. In fact, in the past, Gallo *et al.* have performed interesting studies about the structural changes that NaCl, KCl, and KF provoke in water framed in the context of 'structure making' and 'structure breaking' species [43].

The case of ions consisting of several atoms has been studied much less. The sulfate (SO_4^{2-}) anion is a very interesting case as it is one of the ions available in many minerals on Earth and appears as the second most abundant anion (after Cl^-) in seawater [44]. Understanding the microscopic behaviour of sulfate anions with magnesium, potassium, lithium and sodium cations is useful as they are the most abundant cations in seawater, were it is important to keep the concentration of ions low to maintain the living species. Sulfates play essential roles in environmental chemistry, medicine, industrial processes (like batteries, fertilisers and catalysis), and biological systems. Aqueous sulfate solutions are of particular interest due to their unique physicochemical properties, which influence atmospheric chemistry, water treatment processes, and the behaviour of biological systems [45]. For instance, the role of salt interaction could be important for small biomolecules like aminoacids [46,47]. Furthermore, sulfate aerosols have significant impacts on climate change by affecting the Earth's radiation balance [48]. Additionally, understanding sulfate behaviour in water is critical for understanding processes such as acid rain formation and its subsequent environmental effects [49]. Given their widespread importance, a comprehensive understanding of the behaviour of sulfates in aqueous environments is indispensable for advancements in environmental science, industrial chemistry, and beyond.

In this work, we shall study, using computer simulations, the changes that occur in the structure of water when electrolytes containing the sulfate anion are dissolved.

To perform simulation studies of aqueous electrolyte solutions, one needs to choose a certain force field. As stated previously, one of the fingerprint properties of water is the presence of a maximum in density. A good water model should reproduce this maximum. Although the first generation of water models (TIP3P, TIP4P [50], SPC/E [51]) did not reproduce the temperature at which this maximum occurs (with deviations of 30–40 degrees from the experimental value), the second generation of water models (TIP5P [52], TIP4P-Ew [53], TIP4P/2005 [54]) do indeed reproduce this maximum. In this study, we shall use the TIP4P/2005 model of water as it provides an overall good description of water properties.

In recent years, we have developed a force field for electrolytes in water, denoted the Madrid-2019 force field [55,56]. This force field is especially designed for the TIP4P/2005 model of water. The force field was designed to reproduce the densities and to provide reasonable predictions of transport properties such as viscosities and diffusion coefficients. Additionally, the force field uses a new idea: instead of assigning formal charges to the ions, one uses scaled charges. In particular, for monovalent ions, one will use (0.85 e in electron units) as the charge, and for divalent ions (as is the case of sulfate), one will use a charge of 1.7 e. The idea of using scaled charges was first proposed by Leontyev and Stuchebrukhov and is usually denoted as the Electronic Continuum Correction (ECC) [57–59]. The idea has also been advocated by Vega [60] by stating that different charges should be used to describe the Potential Energy Surface and the Dipole Moment surface. This concept has been followed

by a number of groups, including Jungwirth, Skinner, Barbosa, Predota, among others [61–68]. The ECC correction takes into account that the force field does not include the fast polarisation of electrons that occurs in water when an electric field is applied, which is responsible for the value of 1.78 for the dielectric constant of water at high frequencies of the force field (where electrons but not nuclei have time to react to the field).

It has been shown by several groups that the use of scaled charges improves the description of transport properties [69] and interfacial properties [26]. Recently, we have experimentally determined the maximum in density of a number of ionic solutions at the concentration of 1.00 mol kg^{-1} and compared the results to those obtained by the Madrid-2019 force field (which uses scaled charges) [55], obtaining excellent agreement [70,71]. The agreement was excellent also for salts containing the sulfate anion. Another property that has been measured with this force field for Li_2SO_4 is the freezing point depression, observing that it reproduces the experiments well [26]. Therefore, to study structural changes in water due to the presence of electrolytes, it seems reasonable to select a force field that reproduces the TMD (temperature of maximum density) and the freezing point depression for ionic solutions.

In particular, in this paper, we shall analyse in detail, using computer simulations (with a state-of-the-art force field), the structural changes that occur in the structure of water when adding Na_2SO_4, K_2SO_4, Li_2SO_4, and $MgSO_4$. We shall consider four concentrations (0.64, 1.30, 1.90, and 3 mol kg^{-1}) and two temperatures (300 and 240 K). The choice of a low temperature (in addition to the traditional room temperature) is due to the fact that we want to analyse how the presence of ions modifies the peculiar behaviour of water upon supercooling.

1.1. Model and simulation details

The interactions in the salt aqueous solutions were described using the recently proposed Madrid-2019 model [55]. This force field describes water and the sulfate ions as rigid and non-polarisable. Water is modelled with the TIP4P/2005 potential [54] and ions are represented by Lennard-Jones centres and scaled point charges (0.85 e at the monovalent and 1.7 e at the divalent ions) that, in an effective way, account for the polarisation effects in the solution.

The initial configurations contain 4440 molecules of water and the corresponding amount of ions (Li^+, Na^+, K^+, Mg^{2+} and SO_4^{2-}) depending on the concentration of the solution (m). We studied sulfate aqueous solutions 0.64, 1.30, 1.90 and 3 mol kg^{-1}. The experimental salt solubility in water at 300 K for the studied sulfates is: 1.96 mol kg^{-1} Na_2SO_4, 0.69 mol kg^{-1} K_2SO_4, 3.12 mol kg^{-1} Li_2SO_4 and 3.07 mol kg^{-1} $MgSO_4$ [72,73]. Therefore the highest concentrations studied for the different salts are 3 mol kg^{-1} for Li_2SO_4 and $MgSO_4$ and 1.90 for Na_2SO_4 and K_2SO_4. The edges of the cubic simulation box are approximately $L \approx 5.3$ nm and periodic boundary conditions were applied.

The simulations are performed using the Molecular Dynamics GROMACS 4.5.5 package [74] in the NpT ensemble. The pressure was set to $p = 1$ bar and was controlled using an isotropic Parrinello-Rahman barostat [75], with a relaxation time of 1 ps in the equilibration and 10 ps in the production and a compressibility of 2×10^{-5}. The temperature was set at 300 K and 240 K using the Nosé–Hoover thermostat [76] with a relaxation time of 0.05 ps during the equilibration and 1 ps after the equilibration. The equilibration time was 20 ns and the averages were calculated on production runs of another 20 ns. The equations of motion were integrated using the velocity-Verlet algorithm using a time step of 2 fs. To deal with the long range electrostatic interactions the particle mesh Ewald summations [77] were used. The cut-off distance for the dispersive and the real part of the electrostatic interactions was set to 10 Å. Standard long range corrections were added to energy and pressure for the Lennard Jones part of the potential. The geometry of the water molecules and sulfate ions was constrained with SHAKE (both of them have rigid geometry) [78].

In Figure 1, we compare the densities obtained from our simulations with those obtained for the same model in Ref. [55] (provided in the supplementary material) and with experimental data [79–81]. The agreement between simulations and experiments is excellent.

2. Results

We shall divide the structural results in two parts. First we shall present the results of the structure around the ions of the system. After that we shall analyse how the presence of the ions affects the radial distribution among the atoms of water.

2.1. Hydration coordination layers

2.1.1. Sulfate hydration coordination layer

In Figure 2, we report the behaviour of the sulfur-oxygen (of water O_w) RDF of the sulfate and of the water respectively, $g_{SO_w}(r)$ for ambient temperature and concentration 1.30 mol kg^{-1}. The behaviour of the sulfur-hydrogen RDF of the sulfate and of the water respectively, $g_{SH}(r)$ is reported in Figure 3 and it is quite similar to the one of the $g_{SO_w}(r)$. For both cases we hardly see any change with the concentration of the salt or changing the temperature

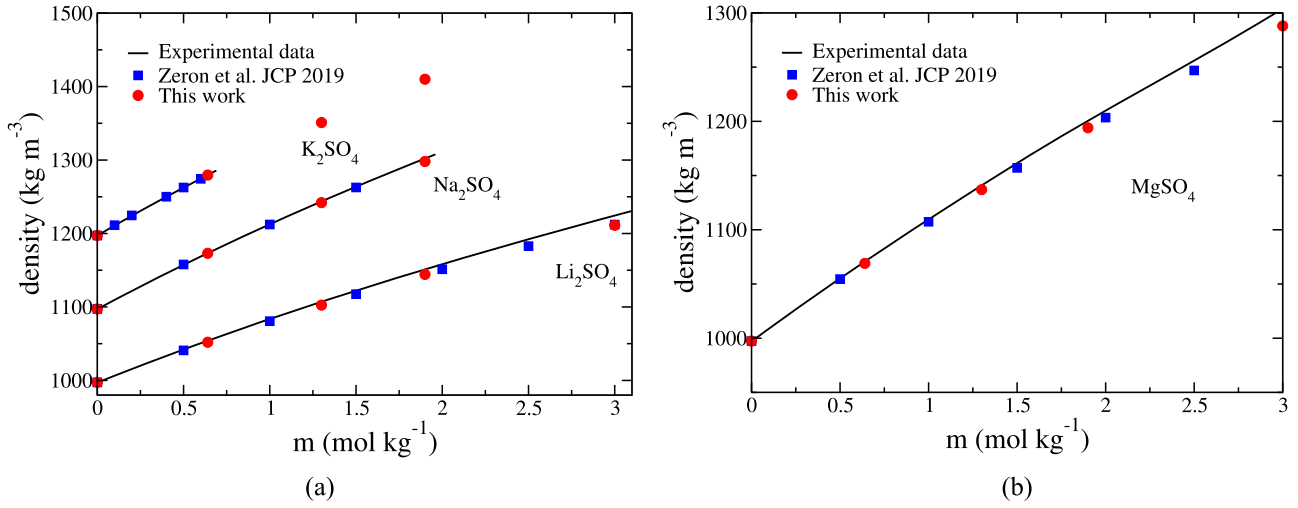

Figure 1. Density as a function of molality for aqueous sulfate solutions at $T = 298.15$ K and $p = 1$ bar. Red dots are the results from this work, the blue squares are from Ref. [55] and the continuous lines are a fit of experimental data taken from Refs. [79–81] and references therein. Na_2SO_4 and K_2SO_4 data are shifted up 100 and 200 kg m^{-3}, respectively.

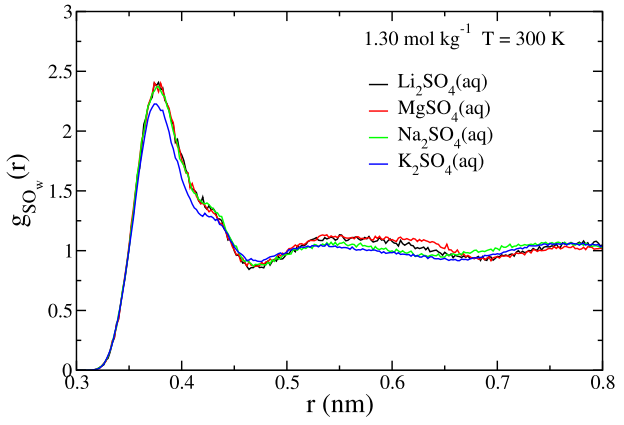

Figure 2. Sulfur-oxygen of water RDF for the studied salts at concentration 1.30 mol kg^{-1}, $p = 1$ bar and 300 K.

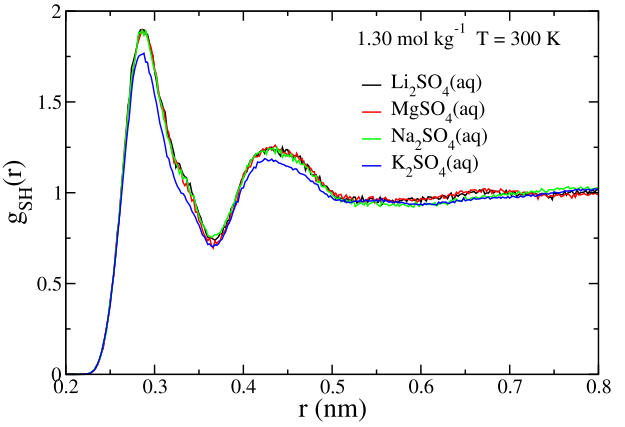

Figure 3. sulfur-hydrogen of water RDF for the studied salts at concentration 1.30 mol kg^{-1}, $p = 1$ bar and 300 K.

and for this reason the graphs comparing temperatures and different concentrations of the salts have been omitted.

As shown in Figure 2, the differences in the $g_{SO_w}(r)$ among various sulfate solutions are quite small. The behaviour of Li and Mg sulfates is almost identical. However, there are some differences for Na and K sulfates. The height of the first peak is noticeably lower for K_2SO_4. The second peak of the correlations for Na_2SO_4 and K_2SO_4 are similar.

To better understand why the first peak height of g_{SO_w} is lower in presence of K^+, we present the S-cation correlation function in Figure 4. Significant differences appear between the different sulfates. The first peak (around 0.35 nm) indicates the presence of contact ion pairs between the sulfate group and the cation, clearly visible for K^+ and Na^+. However, no anion-cation contact pairs exist for Li^+ and Mg^2+. This explains the decrease in the first maximum of S-O_w observed for K^+. In the first hydration layer of the sulfate anion, some cations occupy the position of water in the cases of K_2SO_4 and Na_2SO_4, but not for Li_2SO_4 and $MgSO_4$. However only K_2SO_4 shows a RDF $g_{SK}(r)$ similar to that of $g_{SO_w}(r)$ both in location and shape with a significant and well defined first shell with a shoulder and a well defined second shell so only in the case of of K_2SO_4 we observe a significant presence of the cation in the water solvation shell of the sulfate. The vertical line in Figure 4 shows the border of the water solvation shell. In Figure 5, we plot the g_{SK} together with the sulfate-water g_{SO_W} and g_{SH} and we see how similar is the shape and the first peak location of the g_{SK} to the one of the g_{SO_W} indicating that the K ion, when solvating the sulfate, substitutes a water molecule and lies

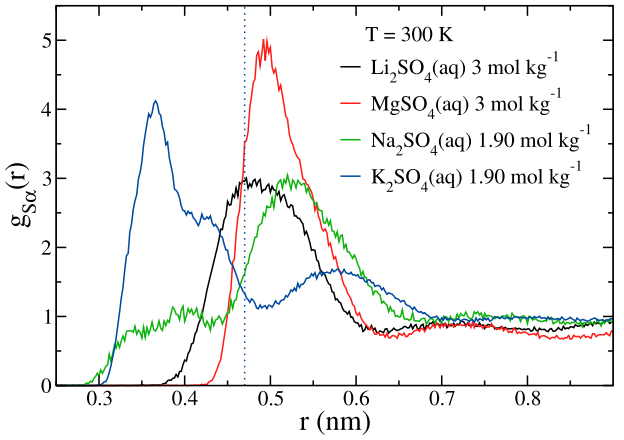

Figure 4. sulfur-cation correlation function at the highest studied concentration of each salt at 300 K and $p = 1$ bar. The doted blue line corresponds to 0.47 nm which corresponds to the minimum of the $g_{SO_w}(r)$ for the K_2SO_4(aq) (hydration solvation shell).

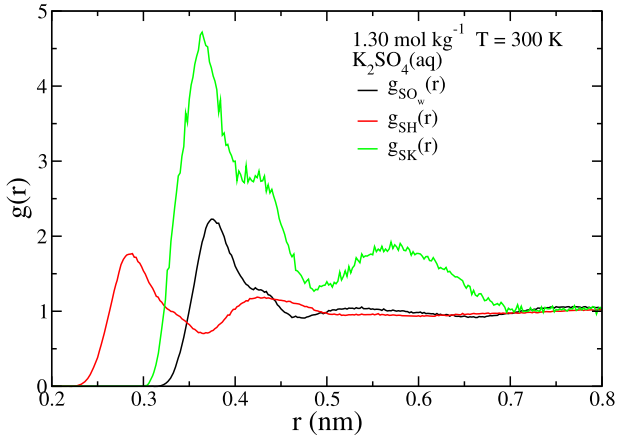

Figure 5. sulfur-oxygen, sulfur-hydrogen and sulfur-cation correlation function at concentration 1.30 mol kg^{-1}, $p = 1$ bar and 300 K for the K_2SO_4.

at the same distance as the oxygens of the water molecules solvating the sulfur, while hydrogen get much closer.

In Table 1, we present the number of contact ion pairs (n^{CIP}). This is typically obtained from the first peak of the radial distribution function between the cation and the anion. However, caution is needed since the first peak of the cation-anion correlation function could correspond to solvent-separated ion pairs (SSIP), where the cation and anion are separated by a water molecule, rather than contact ion pairs (CIP). In this study, Na_2SO_4 and K_2SO_4 form CIP, while Li_2SO_4 and $MgSO_4$ form SSIP. To accurately compute the number of CIP, we integrated the cation-anion correlation function only up to 0.4 nm.

Thus, the number of CIP (n^{CIP}) has been calculated as follows:

$$n^{CIP} = \rho_{SO_4^{2-}} \int_0^{0.4\,nm} 4\pi r^2 g_{S\alpha}(r)\,\mathrm{d}r \qquad (1)$$

Table 1. Number of contact ion pairs (CIP) referred to the sulfate at $p = 1$ bar, for the highest concentration studied for the different salts at 300 and 240 K.

	CIP	
r_{int}	0.4 nm	
T	300 K	240 K
Li_2SO_4(3 mol kg^{-1})	0	0
$MgSO_4$(3 mol kg^{-1})	0	0
Na_2SO_4(1.90 mol kg^{-1})	0.13	0.065
K_2SO_4(1.90 mol kg^{-1})	0.45	0.41

Table 2. Hydration number referred to the sulfate (solvation shell) at $p = 1$ bar, for the highest concentration studied for the different salts at 300 and 240 K. For the first local minimum we used the value $r_{int} = 0.4$ nm.

	Hydration number			
r_{int}	1st local minimum		2nd local minimum	
T	300 K	240 K	300 K	240 K
Li_2SO_4(3 mol kg^{-1})	15.7	15.7	23.1	22.8
$MgSO_4$(3 mol kg^{-1})	15.7	15.7	23.1	22.8
Na_2SO_4(1.90 mol kg^{-1})	15.5	15.5	21.9	22.5
K_2SO_4(1.90 mol kg^{-1})	14.6	14.6	20.7	20.7

where $g_{S\alpha}(r)$ represents the cation-anion radial distribution function. In our analysis we calculated the CIP up to 0.4 nm for all cations. This number is the first minimum of the g_{SK} which is the correlation function of the largest cation.

In addition, the hydration number has been calculated as:

$$n^{hydration} = \rho_{H_2O} \int_0^{r_{int}} 4\pi r^2 g_{SO_w}(r)\,\mathrm{d}r \qquad (2)$$

where $g_{SO_w}(r)$ represents the sulfur-oxygen of the water radial distribution function. Since the first shell of this function shows a shoulder, we calculated the hydration number both for the first local minimum and for the second local minimum. This last integration includes the shoulder.

As confirmed from the number shown in Table 1, K exhibits a significant number of contact ion pairs, while Na shows a small number. No contact ion pairs are observed for Li and Mg. In Table 2, we see that the number of water molecules in the solvation shell has a slight temperature dependence for all cations investigated and it is very similar for all of them except for the K, where we have less water molecules in the solvation shell. By comparing the numbers of Table 2 to those of Table 1 we find them perfectly compatible with the case in which one K replaces one water molecule in the solvation shell of the sulfate. We also note that the decrease of water molecules in the solvation shell due to decreasing temperature happens only for those water molecules residing in the shoulder of the solvation peak.

Coming now back to the behaviour of the $g_{SH}(r)$ correlation function shown in Figure 3 we already observed that this function is quite similar for all the salts, indicating that the cation does not significantly affect the sulfur-H distribution function and therefore the characteristics of the water solvation shell. The first peak occurs at much shorter distances than the sulfur-oxygen radial distribution function, suggesting some weak hydrogen bonding between the hydrogen atoms of water molecules and the oxygens of the sulfate group (the first peak height is not too high). Specifically, the first peak of the $g_{SH}(r)$ occurs around 0.3 nm, while the first peak of the $g_{SO_w}(r)$ is located at 0.4 nm, which is just beyond the OH bond length. This suggests a linear arrangement of the S-O_S vector and the O_w-H vector of the water molecule, forming a linear bridge of the sulfate group with the hydrogens, the difference being the OH bond length). This indicates that sulfate ions can form hydrogen bonds with hydrogen atoms (through its oxygens). The first peak in the $g_{SO_w}(r)$ is around 0.4 nm, so it is at a distance of almost 0.1 nm from the one in the $g_{SH}(r)$, this could show the tendency of the hydrogens to form practically linear bridges between the oxygens of water and the sulfate group. We already observed that the only salt with different behaviour is K_2SO_4 being the height of the first peak lower than for the other salts. As described above, this is due to the existence of contact ion pairs in K_2SO_4, where some K cations lie the water solvation shell and are in contact with the oxygens of the sulfate group.

From the results shown it can be inferred that the difference in behaviour of the K^+ with respect to the other cations studied appears due to the fact that K^+ has not only the larger ionic radius but also a diameter similar to the O^{2-} and the K^+, resulting in the first peak of the $g_{KO_w}(r)$ overlapping with the one of the $g_{O_wO_w}(r)$.

2.1.2. Cation hydration coordination layer

In Figure 6, we present the behaviour of the cation-oxygen of water RDF, $g_{ZO_w}(r)$. The abscissa is rescaled with the distance of the maximum of the peak of the $g_{ZO_w}(r)$, r_{ZO_w}, to facilitate the comparison between different ions. Table 3 reports the values of the positions of the first peak of the $g_{ZO_w}(r)$. We observed that the position of the first peak does not change with increasing ion concentration or changing temperature for both $g_{ZO_w}(r)$ and $g_{ZH}(r)$ (graphs not included). However, the height of the first peak becomes somewhat higher at lower temperatures.

As can be seen, the hydration of water around the ion is strong. However, significant differences are found between different cations. Li^+ and Mg^{2+} seem to belong to one group, while Na^+ and K^+ belong to another. The height of the first peak decreases in the order: $Mg^{2+} > Li^+ > Na^+ > K^+$. This aligns with the charge density of the cation (i.e. the charge of the ion divided by the volume). Specifically, the charge density decreases in the order: $Mg^{2+} > Li^+ > Na^+ > K^+$.

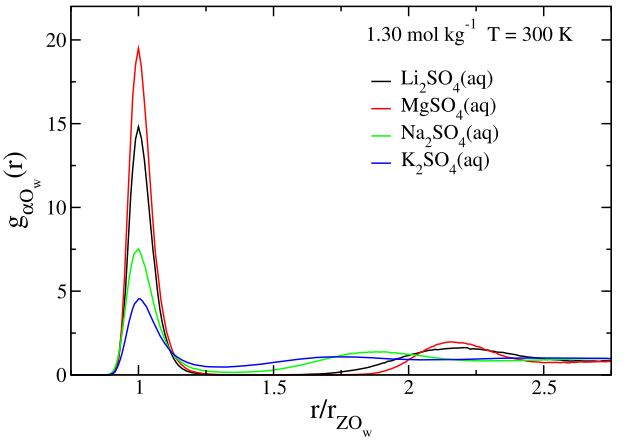

Figure 6. Cation-oxygen of water RDF for the studied salts at concentration 1.30 mol kg^{-1}, $p = 1$ bar and 300 K.

Table 3. Positions of the first peak of the cation-oxygen of water RDF at $p = 1$ bar, it does not change with concentration and temperature.

	r_{ZO_w} (nm)
Li_2SO_4(aq)	0.184
$MgSO_4$(aq)	0.192
Na_2SO_4(aq)	0.234
K_2SO_4(aq)	0.272

The electric field produced by a small ion with a large charge, such as Mg, is substantial, forcing water molecules to locate close to it. The ratio of the height of the first peak between Mg and K is a factor of four. Thus, Mg^{2+} and K^+ have quite different effects on water, particularly in the first solvation shell. Not only is the height of the first peak different, but so is the height of the second peak. The second peak is higher for Mg^{2+}/Li^+ than for Na^+/K^+, indicating that Mg and Li affect the structure of water in both the first and second solvation shells.

For a 1.30 mol kg^{-1} solution, there are about 21 molecules of water per ion, roughly the number of water molecules in two coordination shells. This suggests that the impact of Li^+ and Mg^{2+} on the structure of water is dramatic.

The (higher) the first peak, the narrower the second hydration shell appears to be. This suggests that magnesium cations enforce greater orientational ordering of water molecules in the first two hydration shells compared to other cations.

In Figure 7, we present the cation-hydrogen RDF, $g_{ZH}(r)$, scaled by the distance of the first peak of the cation-oxygen correlation function. This function reveals

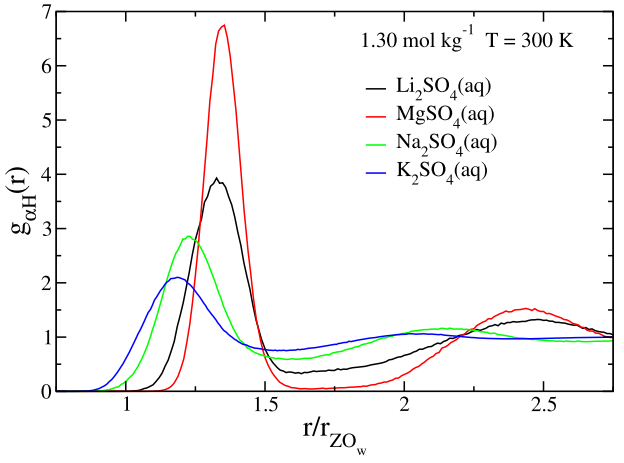

Figure 7. Cation-hydrogen RDF for the studied salts at concentration 1.30 mol kg^{-1}, $p = 1$ bar and 300 K.

insightful aspects about the orientation of water in the cation's first hydration layer.

If water molecules in the first hydration layer align their dipole moments with the cation-oxygen vector, one would expect the first peak of the cation-H distribution function to appear at longer distances. Conversely, if these water molecules can rotate, the first peak would shift to shorter distances. This behaviour is clearly observed in Figure 7.

Li_2SO_4 and $MgSO_4$ exhibit peaks at longer distances, indicating rigid orientation of water molecules with their dipole moments aligned with the cation-oxygen vector. In contrast, Na_2SO_4 and especially K_2SO_4 show broader peaks at shorter distances, suggesting a higher degree of rotational freedom for water molecules in their first hydration shell.

Thus, the presence of cations affects not only the spatial arrangement of water molecules but also their orientation in the first hydration shell. Li^+ and Mg^{2+} rigidly fix both the position and orientation of water molecules in this shell, while Na^+ and K^+ primarily fix the position but allow for rotational freedom. This distinction underscores that Li^+ and Mg^{2+} exert greater control over the structure of water, at least within the first solvation shell, compared to Na^+ and K^+. Furthermore, the orientation of water molecules in the first solvation shell influences the positioning of molecules in the second shell to maintain the typical hydrogen bonding network of water.

Another indirect method to assess changes induced by ions in the structure of water involves evaluating the potential energy between water molecules. In pure water, the primary contribution to potential energy arises from hydrogen bonds between water molecules, which can be rationalised by the high vaporisation enthalpy of about 44 kJ mol^{-1}. This value corresponds to each water molecule forming approximately two hydrogen bonds, each with an energy of around 22 kJ mol^{-1}.

Table 4. Water-water potential energy (U) for the different salt solutions with a concentration of 1.90 mol kg^{-1} studied at 300 K and $p = 1$ bar.

	U (kJ mol^{-1})
$MgSO_4$(aq)	−20.83
Li_2SO_4(aq)	−27.13
Na_2SO_4(aq)	−28.85
K_2SO_4(aq)	−32.25

Therefore, it is valuable to determine the potential energy between water molecules (excluding interactions with ions or between ions) in aqueous electrolyte solutions. Naturally, this energy is expected to be lower than in pure water due to water molecules being in proximity to ions, thereby reducing water-water interactions. However, differences in water-water potential energy may exist among different salts at the same concentration.

In Table 4, we present these potential energy values for water. K_2SO_4 exhibits the lowest potential energy, indicating minimal modification of water structure, followed by Na_2SO_4 and Li_2SO_4, which show higher water-water potential energies. $MgSO_4$ demonstrates the highest value, even considering that a 1.90 mol kg^{-1} solution of this salt contains fewer ions than monovalent cation salts like Na_2SO_4. Given that the anion is sulfate across all cases, these differences are attributed to the cation.

As cation charge density increases (charge divided by cation volume), disruption of the water-water hydrogen bonding structure also intensifies. Cations with higher charge densities exert stronger geometric demands on water molecules, hindering their ability to satisfy the natural propensity for hydrogen bonding among themselves.

From the findings in Table 4, it can be concluded that changes in water structure follow the order $MgSO_4 > Li_2SO_4 > Na_2SO_4 > K_2SO_4$. This order is in agreement with the experimental values of the hydration Gibbs free energies of the chlorine salts with the corresponding cations. The values are: −2580 kJ mol^{-1} for $MgCl_2$, −815 kJ mol^{-1} for LiCl, −705 kJ mol^{-1} for NaCl, and −635 kJ mol^{-1} for KCl [82].

In Table 5, the ion-water energy (per ion) is shown for solutions with a concentration 1.90 mol kg^{-1}. As it can be seen, the energy of the sulfate group with water does not depend on the cation and it remains approximately constant. Only in the case of the salt containing potassium the energy is somewhat smaller (in absolute value). This is due to the fact that some K^+ are in contact with the sulfate thus replacing water in the first hydration layer. Concerning the energy of the cations with water all values are negative. The absolute value is quite large in the case of Mg^{2+}, large in the case of Li^+, moderate in the case

Table 5. Cation-water and SO_4^{2-}-water energy (Lennard-Jones plus Coulombic energy) divided by the number of cations or anions respectively, for the different salt solutions with a concentration of 1.90 mol kg^{-1} studied at 300 K and $p = 1$ bar.

	Cation-water energy (kJ mol^{-1})	SO_4^{2-}-water energy (kJ mol^{-1})
$MgSO_4$(aq)	−1258	−468
Li_2SO_4(aq)	−471	−471
Na_2SO_4(aq)	−221	−462
K_2SO_4(aq)	−115	−403

of Na^+ and small in the case of K^+. Thus it means that the strength of the hydration of water around the cation decreases in the order Mg^{2+}, Li^+, Na^+ and K^+. This can be understood as the charge of the Mg^{2+} is twice that of the rest of the cations charge. In the case of monovalent cations the hydration strength decreases as the size of the cation increases (defining the size of the cation as the distance of the first peak of the cation-O_w radial distribution function).

2.2. Water structure

2.2.1. Water's oxygen structure

Here we discuss the effect of different sulfate salts and their concentrations on the structure of water at two temperatures: 300 and 240 K. To do this, we begin by presenting the radial distribution functions of the oxygens in the water, $g_{O_wO_w}(r)$, shown in Figure 8. We observe increased perturbations in the $g_{O_wO_w}(r)$ with increasing salt concentration. Generally, these changes are even more noticeable at the lower temperature of 240 K.

For Li_2SO_4, Na_2SO_4, and K_2SO_4 at 1.90 mol kg^{-1} aqueous solutions, the observed perturbation in the $g_{O_wO_w}(r)$ upon dissolving these salts seems to indicate a decrease in the structural order of water. Specifically, the height of the first peak decreases with increasing salt concentration, and the value of the first minimum increases with increasing salt concentration in a monotonous way.

The signatures of tetrahedral order, such as those seen in low-density amorphous (LDA) ice and in supercooled water [11], are high values of the first peak and low values of the first minimum.

Thus, it is clear that the presence of salt disrupts the tetrahedral order of water, with the change being continuous with concentration. The addition of salt shows similar behaviour to that observed when increasing pressure on pure water, which also leads to an increase in distorted tetrahedra [39].

The behaviour of $MgSO_4$ in water is distinct from that of the other salts. Notably, the height of the first peak increases with the concentration of $MgSO_4$, and this perturbation is not enhanced at lower temperatures. At ambient temperature, there is no significant change in the first minimum with varying salt concentration. Another observed perturbation is the appearance of a new second peak around 0.38 nm, accompanied by the progressive disappearance of the second coordination layer present in pure water. This last effect is similar to what is observed with the other sulfates.

Table 6. Positions of the first peak of the oxygen-oxygen of water RDF at $p = 1$ bar, for the studied salt solutions with a concentration of 1.90 mol kg^{-1}.

	300 K		240 K	
	$r_{O_wO_w}$ (nm)	$g_{O_wO_w}(r)$	$r_{O_wO_w}$ (nm)	$g_{O_wO_w}(r)$
water	0.278	3.22	0.276	4.15
Li_2SO_4(aq)	0.280	2.87	0.276	3.46
$MgSO_4$(aq)	0.276	3.89	0.276	4.65
Na_2SO_4(aq)	0.278	2.78	0.276	3.32
K_2SO_4(aq)	0.277	2.96	0.276	3.90

Table 7. Positions of the first minimum of the oxygen-oxygen of water RDF at $p = 1$ bar, for the studied salt solutions with a concentration of 1.90 mol kg^{-1}. Results for Na_2SO_4(aq) are not shown as we can not detect a clear minimum in the radial distribution function.

	300 K		240 K	
	$r_{O_wO_w}$ (nm)	$g_{O_wO_w}(r)$	$r_{O_wO_w}$ (nm)	$g_{O_wO_w}(r)$
water	0.330	0.754	0.327	0.405
Li_2SO_4(aq)	0.351	0.862	0.336	0.681
$MgSO_4$(aq)	0.329	0.823	0.318	0.590
K_2SO_4(aq)	0.329	1.01	0.320	0.688

As common knowledge would suggest, in all cases, we observe a higher first peak for the $g_{O_wO_w}(r)$ at lower temperatures, indicating a more ordered structure. This is clearly seen in Table 6, where the height of the first peak of the oxygen-oxygen distribution function of water is shown for both temperatures. In Table 7, the location and value of the radial distribution function at the first minimum are shown. As can be seen for all salts (with the exception of Na_2SO_4, where no clear minimum is observed), the value of the first minimum decreases significantly when the temperature decreases to 240 K.

Now, let us compare the behaviour of the oxygen-oxygen distribution of water and the oxygen-hydrogen distribution for a fixed concentration. In Figure 9, we compare the $g_{O_wO_w}(r)$ of the studied salt solutions at a concentration of 1.90 mol kg^{-1}. The height of the first peak of the O_w-O_w RDF for $MgSO_4$ is much higher than that for the rest of the salts, which is related to its nature of divalent cation.

Interpreting the first minimum is more challenging. For Na_2SO_4, it seems that some water molecules are in contact but not forming hydrogen bonds (explaining the maximum at around 0.33 nm). For K_2SO_4, there appears to be no distinct first minimum or second maximum, resulting in a very flat structure beyond the first hydration shell.

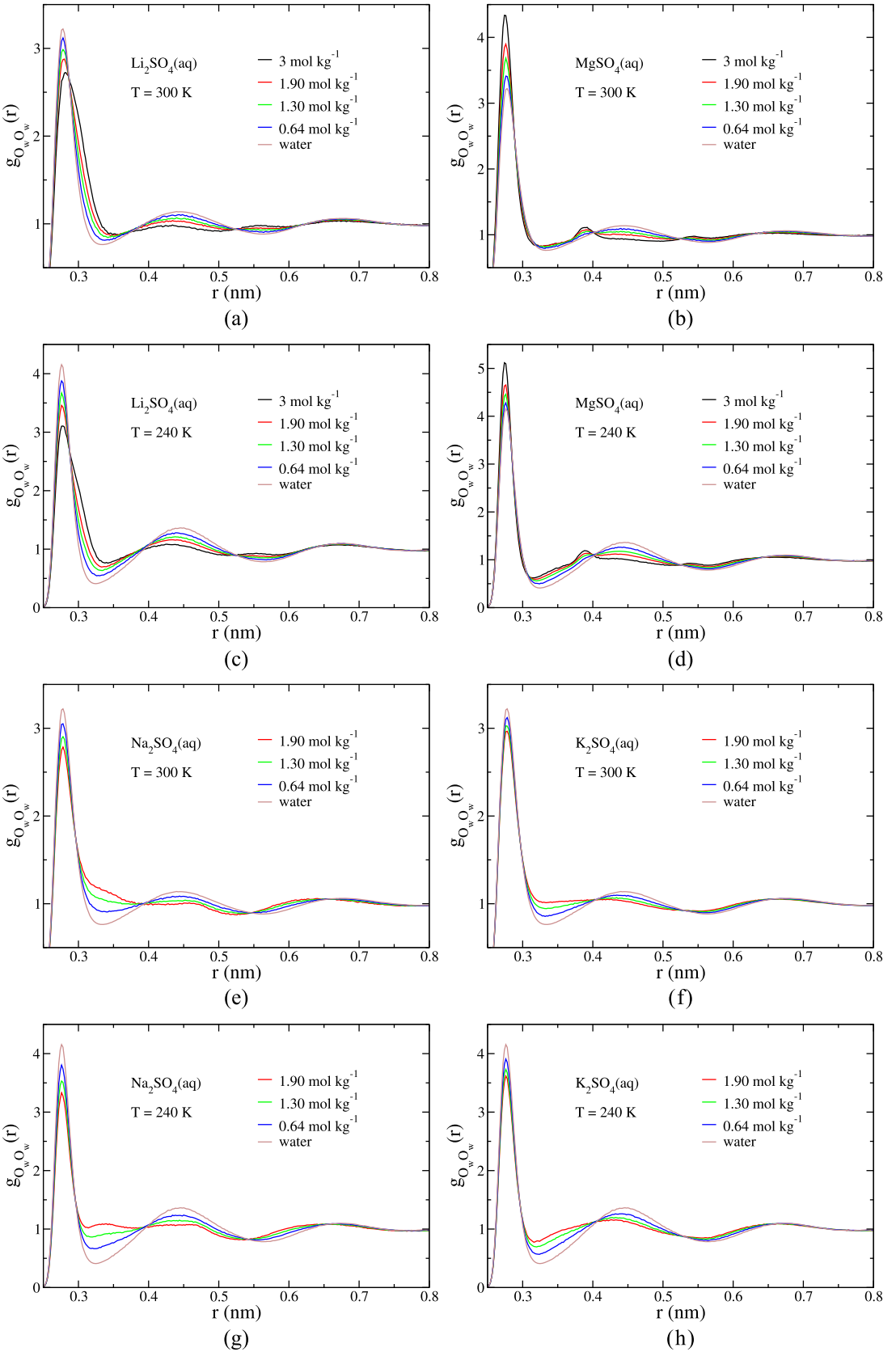

Figure 8. Oxygen-oxygen RDF of waterat $p = 1$ bar. (a) Li_2SO_4 at 300 K. (b) $MgSO_4$ at 300 K. (c) Li_2SO_4 at 240 K. (d) $MgSO_4$ at 240 K. (e) Na_2SO_4 at 300 K. (f) K_2SO_4 at 300 K. (g) Na_2SO_4 at 240 K and (h) K_2SO_4 at 240 K.

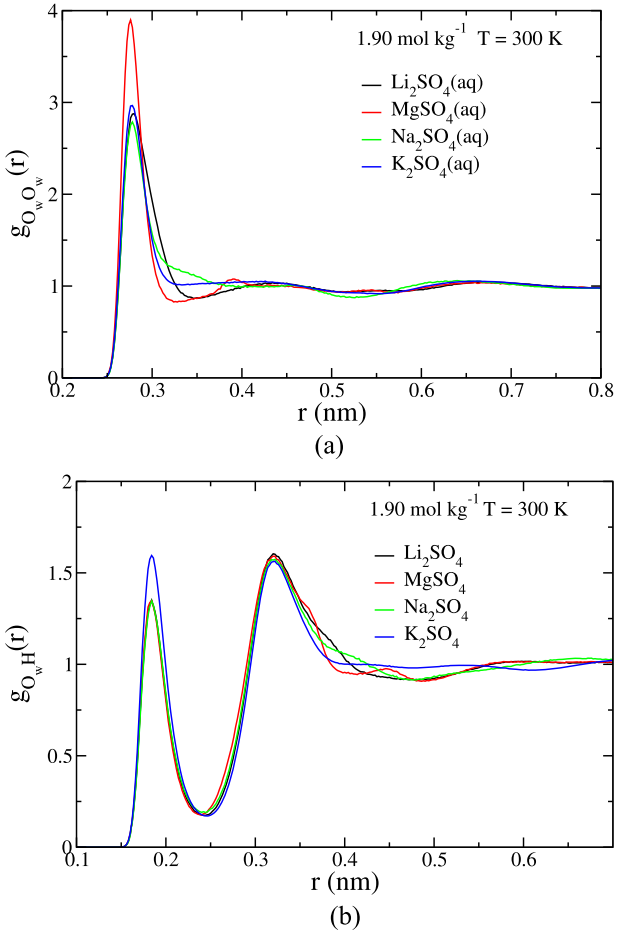

Figure 9. (a) Oxygen-oxygen RDF of water and (b) Oxygen-hydrogen RDF of water for different salts at concentration 1.90 mol kg^{-1}, at $p = 1$ bar and 300 K.

Regarding the O_w-H distribution function, the first peak (reflecting hydrogen bonding) is much higher for K_2SO_4 than for any other salt, explaining why the water-water potential energy of this salt reached the lowest value, as discussed previously. Another surprising behaviour is that for K_2SO_4, the distribution function is uniform beyond 0.4 nm. This suggests that in the salt containing K, each water molecule forms strong hydrogen bonds with its nearest neighbours, but the structure beyond the first hydration layer is rather weak. This is evident in both the O_w-O_w and O_w-H distribution functions.

2.2.2. Local structure

To check the oxygen's water structure order with a higher accuracy, we analysed two local structure parameters. The first one is the orientational order parameter q_t proposed by Errington and Debenedetti [83] and defines as follows:

$$q_t = 1 - \frac{3}{8}\sum_{i=1}^{3}\sum_{j=i+1}^{4}\left(\cos(\gamma_{ij}) + \frac{1}{3}\right)^2 \qquad (3)$$

where one oxygen is considered with its four nearest neighbours. $\gamma\, ij$ is the angle formed by the lines joining the oxygen considered and two of its four nearest neighbours. Given its definition q_t is sensitive to the angular distribution of the water molecules in the first shell.

The second parameter is the cosine of the O-O-O angle averaged over neighbours within 3.5 Å, which will be denoted as $\cos\gamma$.

The results for these two local structural orientational order parameters are shown in Figure 10 and in Figure 11 for all the solutions investigated at the various concentrations and for both temperatures. Results are always compared with those of the bulk phase at the same thermodynamic conditions.

In Figure 10, we show the probability distribution of q_t. The bulk distribution is characterised by one peak close to 1 and one shoulder around 0.5. A perfect tetrahedral arrangement corresponds to $q_t = 1$. The shoulder of the bulk phase is the signature of interstitial water and therefore of HDL local configuration while the peak close to one is the signature of LDL local structures. Upon cooling we see that in the bulk the LDL peak enhances consistently at the expenses of the shoulder that almost disappears.

At 0.64 mol kg^{-1} water in the solutions investigated shows a behaviour similar to the bulk only with a lower LDL peak and a higher HDL peak. As the concentration of the ions is increased in the sulfate aqueous solutions q_t shifts to lower values while the tetrahedral peak decreases showing the gradual loss of local tetrahedral structure of the water oxygens, that we already pointed out from looking at the $g_{O_wO_w}(r)$s. We also observe that the behaviour of water in the solutions is quite similar for those containing the Na and K cations. They both show only two peaks, as in the bulk phase, although the peak associated with HDL water is enhanced and shifted to lower values of q_t showing that the HDL water structure is still there but distorted. The solutions containing Li and Mg show a similar behaviour but also the appearance of new peaks at lower values of q_t signalling new local configurations for water. In particular for the case of Li_2SO_4 one new peak appears and for the case of $MgSO_4$ two new peaks appear.

Upon cooling we nonetheless note for all the solutions investigated that the LDL peak enhances showing that in spite of the perturbation due to the presence of the ions water still retains its tendency to form LDL upon cooling. And this is true also for $MgSO_4$ solutions that show the biggest modification respect pure water.

In Figure 11, we show the probability distribution of the cosine of the O-O-O angle. The bulk distribution is characterised by a peak around 0.63 which is related to interstitial water and therefore to the presence of HDL configurations and a very broad peak centred

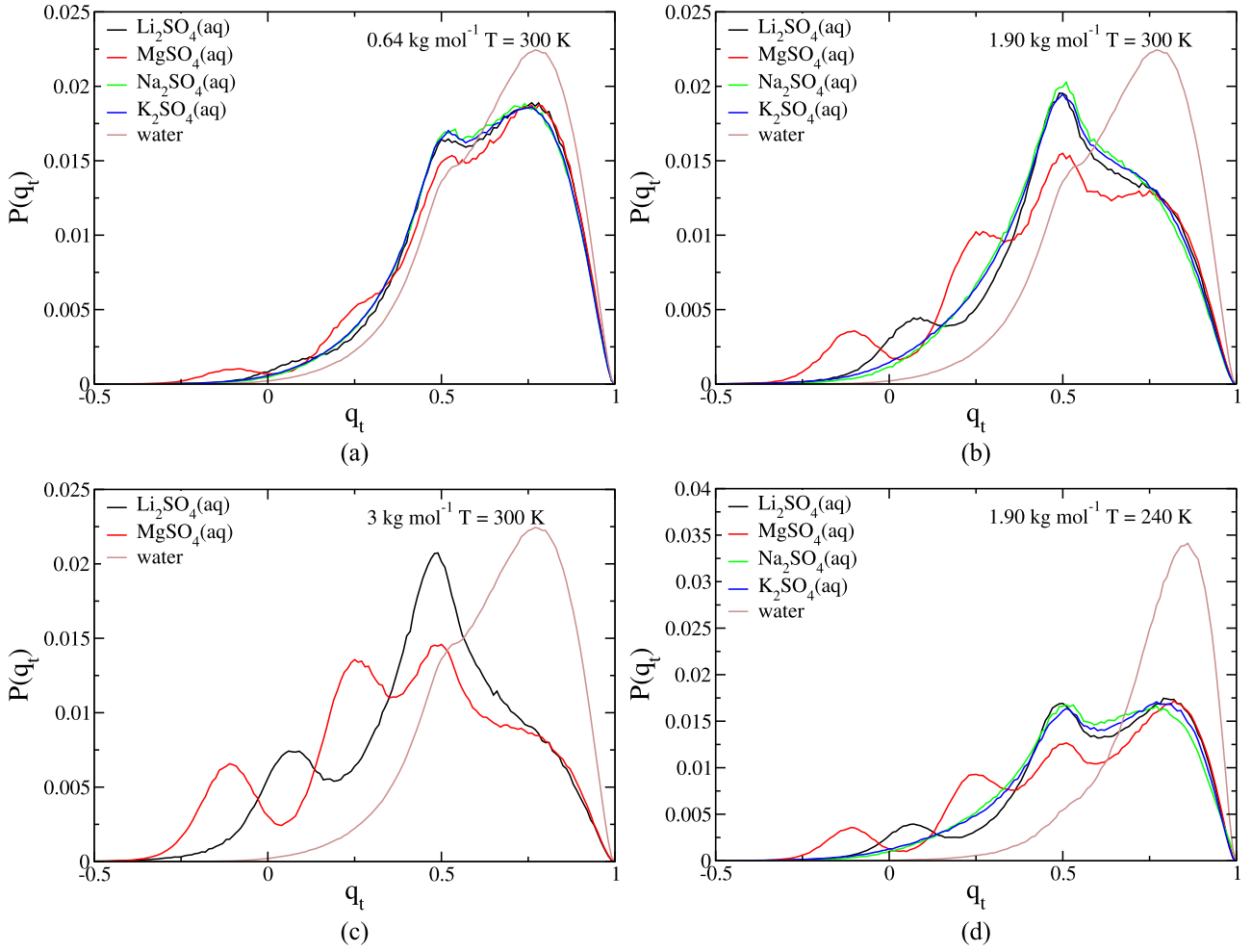

Figure 10. Probability distribution of the orientational order parameter q_t at $p = 1$ bar. On the left we show the distributions for sulfates at 300 K (a) for sulfates at 0.64 mol kg^{-1} and (c) for sulfates at 3 mol kg^{-1} in order to appreciate the effect of the increase of concentration (we do not include K_2SO_4 nor Na_2SO_4 because their experimental solubility is much lower than 3 mol kg^{-1}). On the right we show the distributions for the sulfates at 1.90 mol kg^{-1} for (b) 300 K and (d) 240 K in order to appreciate the effect of the decrease of the temperature.

around −0.25 corresponding to the tetrahedral order. In general, the height increases and the minimum depth decrease when adding sulfates, they also appear to be shifted towards smaller $\cos\gamma$. Already at 0.64 mol kg^{-1} the $MgSO_4$ induces a higher perturbation in the oxygens of water, since it gives birth to a new peak when the cosine is 0 corresponding to an angle of $\pi/2$ among the three oxygens. This is in agreement to what we observed on Figure 9 and Table 6, where we observed the highest distortion of the first peak for Mg^{2+}. Upon increasing concentration of ions Li and Mg show a strong enhancement and a shift of the peak of interstitial water while Na^+ shows oscillations similar to Mg^{2+} upon enhancing concentration and especially upon cooling. Also for this local structure parameter we observe, nonetheless, that water still shows a tetrahedral character that enhances upon cooling. We also note that, especially upon supercooling, the smallest perturbation of water structure appears to be induced by the solutions containing the K counterion which we already noted that is more affine to the water oxygen in size.

2.2.3. Hydrogen bond network

Following we can discuss the effect on the hydrogen bond network (HBT) by observing the $g_{O_wH}(r)$ and $g_{HH}(r)$, in Figures 12 and 13 respectively.

When adding sulfates, the HBT seems to be less affected than the oxygen structure. However, also in this case the effect is more notorious at lower temperature. In both Figures 12 and 13, we observe a decrease in the height of the first peak when adding more salt, the first minimum depth is kept but it moves slightly closer to the first peak.

The second peak of the OO RDF does not seem to be almost affected. But for the $g_{HH}(r)$ the second minimum changes. Meaning that for a concentration of 3 mol kg^{-1} a

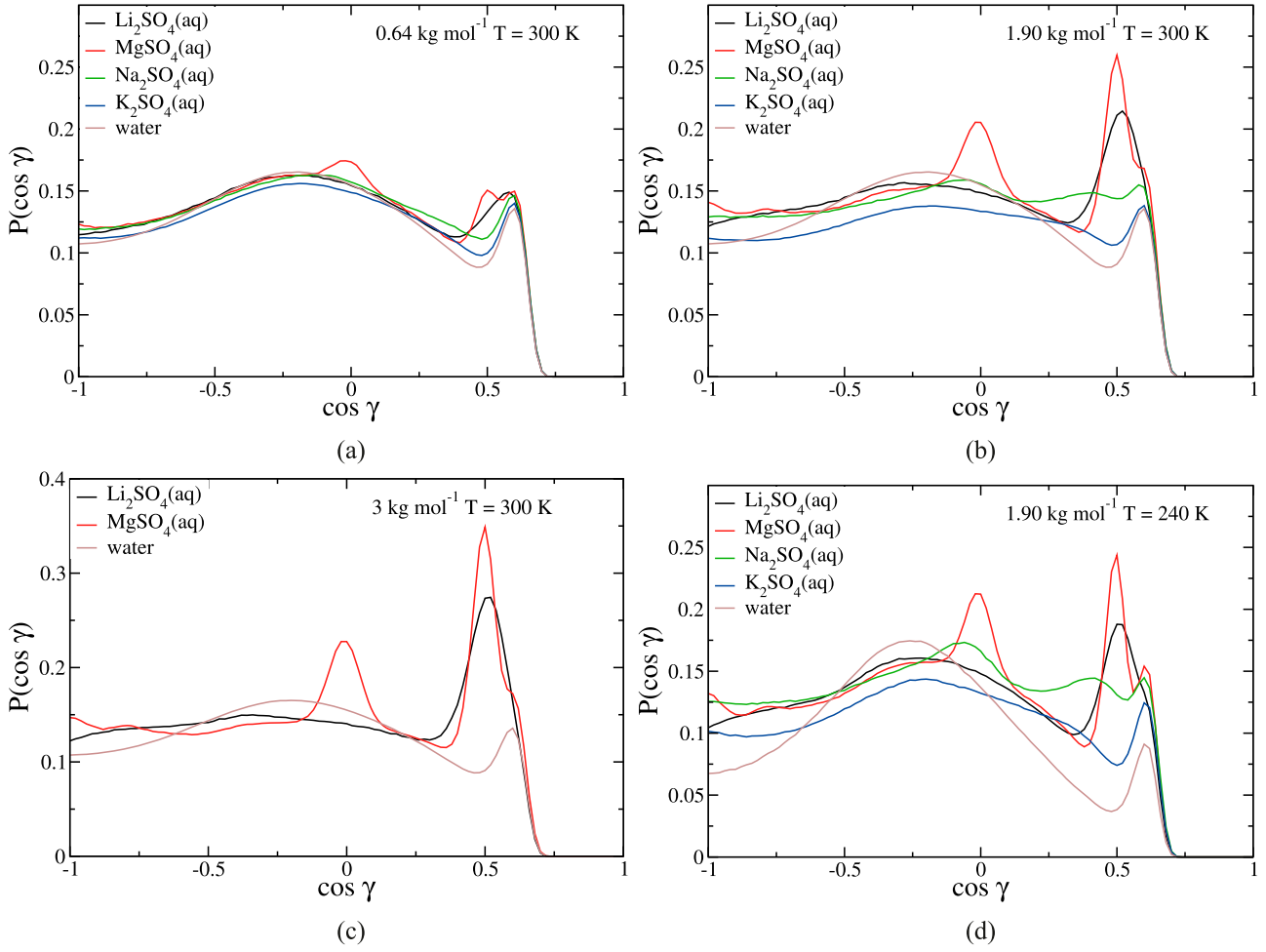

Figure 11. Probability distribution of the O-O-O angle averaged over neighbours within 3.5 Å at $p = 1$ bar. On the left we show the distributions for sulfates at 300 K (a) for sulfates at 0.64 mol kg^{-1} and (c) for sulfates at 3 mol kg^{-1} in order to appreciate the effect of the increase of concentration (we do not include K_2SO_4 nor Na_2SO_4 because their experimental solubility is much lower than 3 mol kg^{-1}). On the right we show the distributions for the sulfates at 1.90 mol kg^{-1} for (b) 300 K and (d) 240 K in order to appreciate the effect of the decrease of the temperature.

new peak starts appearing at close to the second one, and the minimum gets deeper and new peaks start appearing after the cited ones.

Analogously to the situation for the $g_{O_wO_w}(r)$, the K_2SO_4 aqueous solution at 1.90 mol kg^{-1} presents an anomaly for the $g_{O_wH}(r)$, since it seems to have the opposite effect on the water's oxygens structure than lower concentrations.

A similar distortion is observed when increasing pressure on pure water [14,39]. According to Soper and Ricci, HDL water is characterised by the persistence of the HBT and a broadening of the second peak of the $g_{O_wO_w}(r)$ [11]. Following this observations, we could understand the effect of adding salt to water as a continuous change of the water structure towards the HDL structure, as it was also observed for NaCl, KCl and KF aqueous solutions by Gallo *et al.* [43].

2.2.4. Diffusion of water

In Figure 14 and Table 8, we report the diffusion coefficients, D, for the oxygens in the water molecules with different concentrations of the studied salts at two temperatures. At 300 K, we observe that diffusion decreases with increasing salt concentration. It is interesting to note that K_2SO_4 has a milder effect compared to the other three salts.

A similar behaviour was observed for NaCl, KCl, and KF aqueous solutions by Gallo *et al.* [43] and when increasing pressure on bulk water [84,85].

However, there is a surprising behaviour at 240 K. The sulfate salts containing Li, Na, and Mg behave similarly, but the decrease in the diffusion coefficient of water with increasing salt concentration is much smaller than at room temperature. Even more surprising, in the case of the sulfate solution containing K, the diffusion

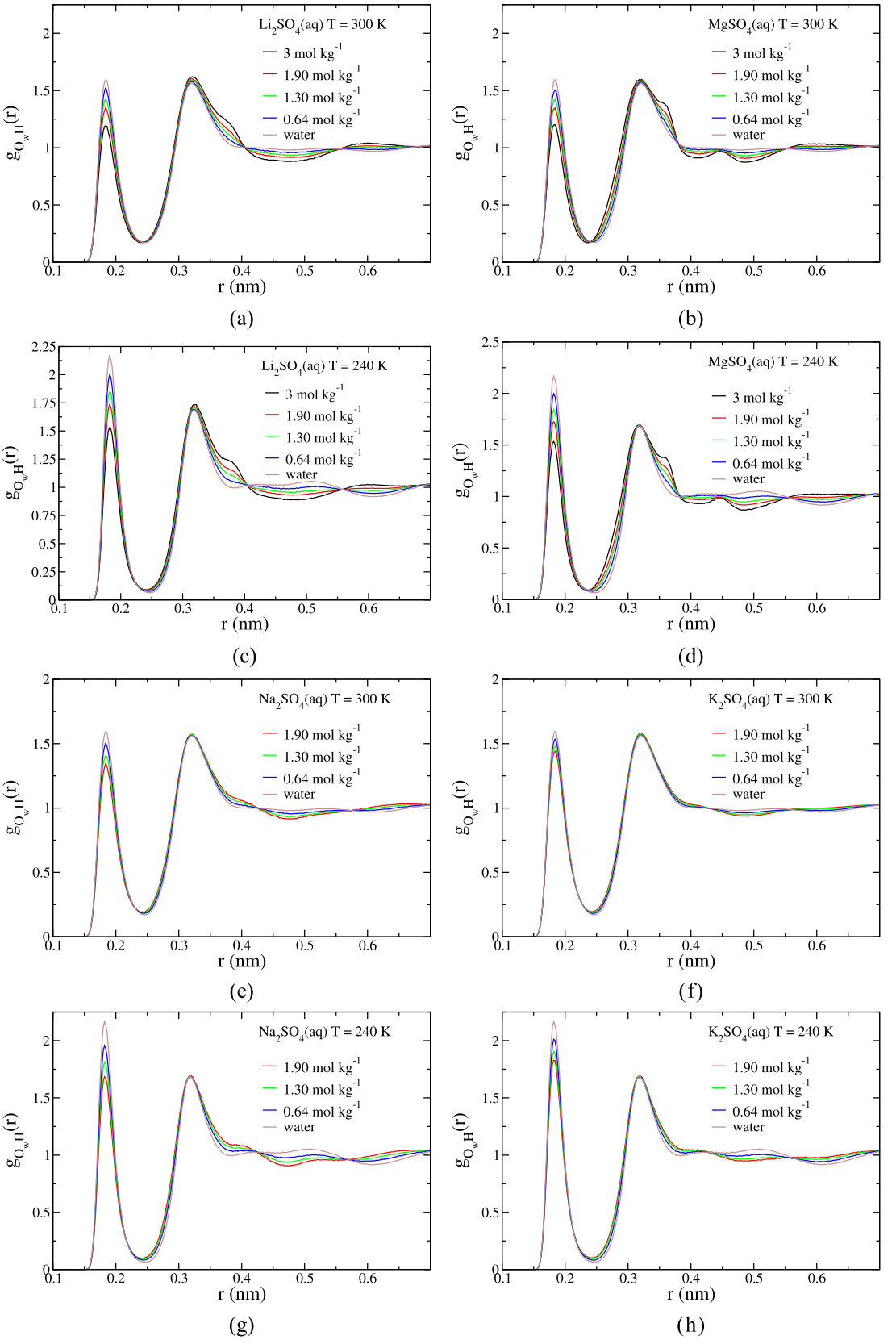

Figure 12. Oxygen-hydrogen RDF of water at $p = 1$ bar. (a) Li_2SO_4 at 300 K. (b) $MgSO_4$ at 300 K. (c) Li_2SO_4 at 240 K. (d) $MgSO_4$ at 240 K. (e) Na_2SO_4 at 300 K. (f) K_2SO_4 at 300 K. (g) Na_2SO_4 at 240 K and (h) K_2SO_4 at 240 K.

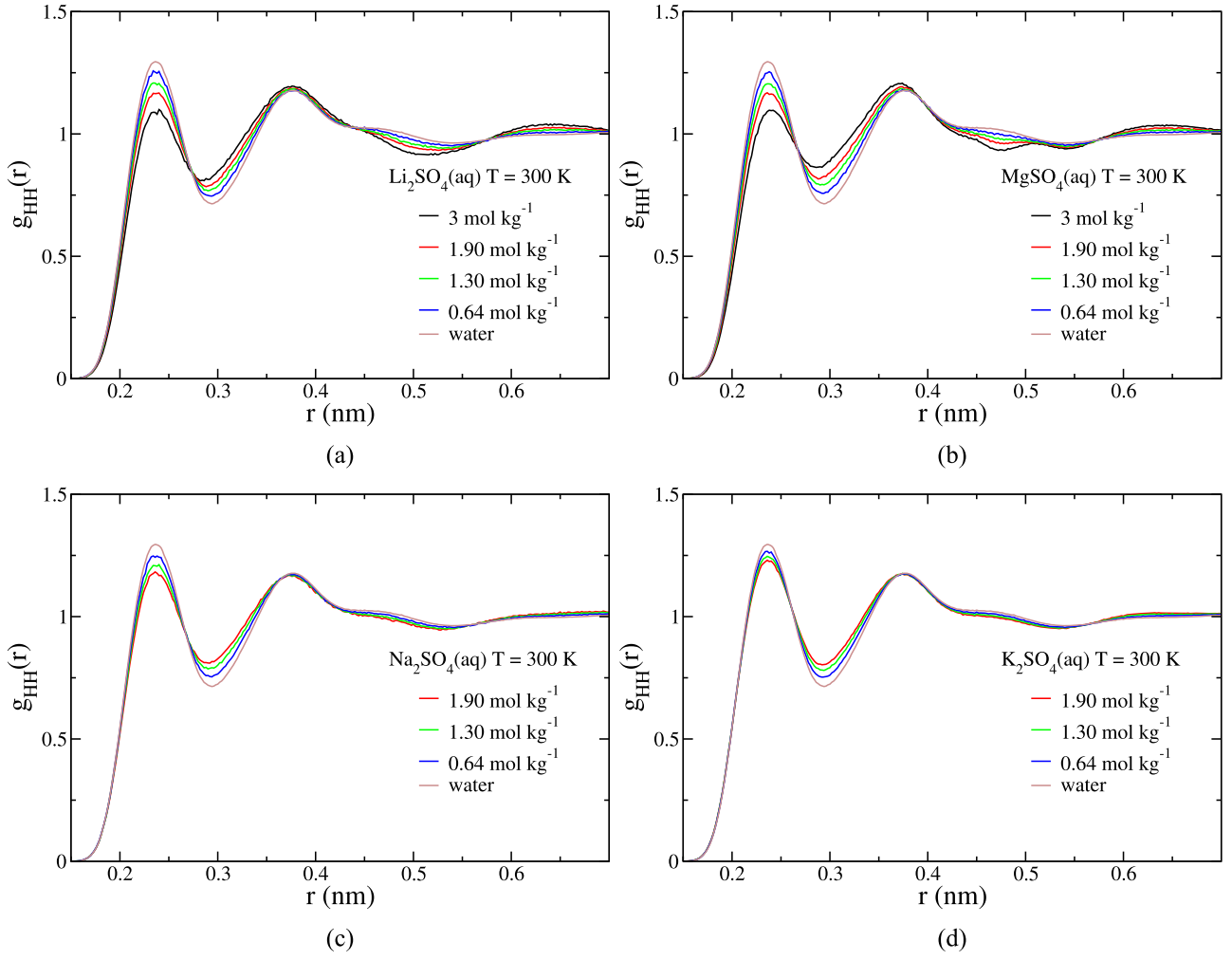

Figure 13. Hydrogen-hydrogen RDF of water at $p = 1$ bar and 300 K. (a) Li_2SO_4. (b) $MgSO_4$. (c) Li_2SO_4 and (d) $MgSO_4$.

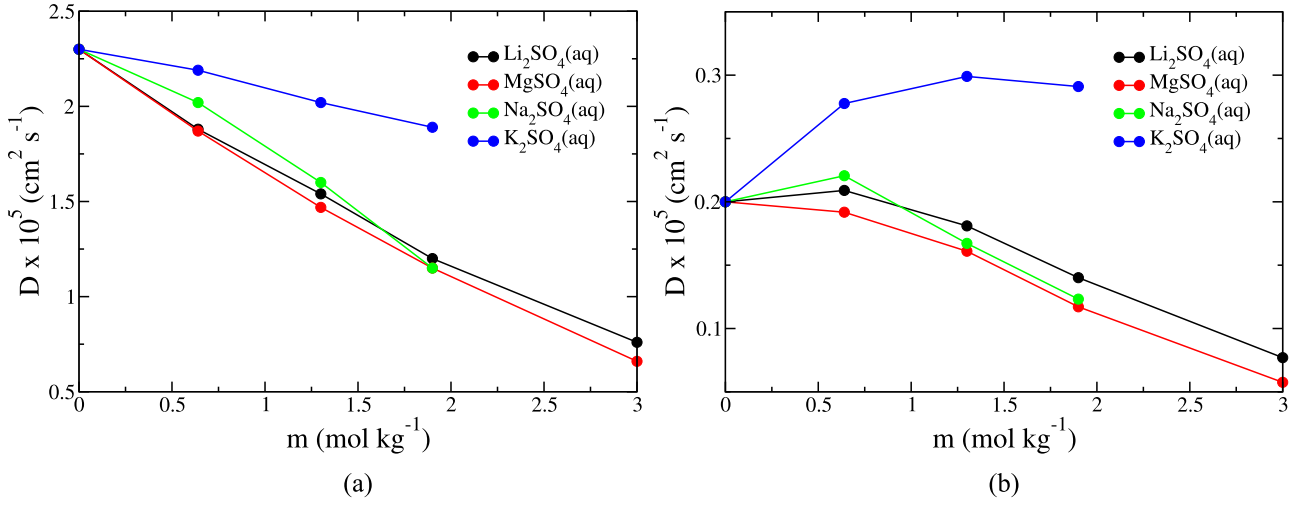

Figure 14. Diffusion coefficient of water's oxygen at (a) 300 K and (b) 240 K for aqueous solutions of different sulfates at different concentrations and $p = 1$ bar.

coefficient of water increases as salt is added, at least for concentrations up to 2 mol kg^{-1}. Water accelerates as salt is added. This behaviour could be related to the water density anomaly when taking into account that water in presence of ions has a higher density with respect to the bulk at the same thermodynamic conditions [86].

Table 8. Diffusion coefficient of the oxygen belonging to water for bulk TIP4P-2005 water and aqueous solutions of different sulfates at different concentrations and temperatures and $p = 1$ bar.

	$D_{H_2O} \times 10^5$ cm^2 s^{-1}			
m mol kg^{-1}	Li_2SO_4(aq)	$MgSO_4$(aq)	Na_2SO_4(aq)	K_2SO_4(aq)
T = 300 K				
0	2.30(8)			
0.64	1.88(4)	1.87(3)	2.02(7)	2.19(3)
1.30	1.54(3)	1.469(6)	1.60(3)	2.02(9)
1.90	1.20(1)	1.15(4)	1.31(2)	1.89(2)
3	0.76(1)	0.66(3)		
T = 240 K				
0	0.200(2)			
0.64	0.209(4)	0.1918(10)	0.2206(6)	0.278(2)
1.30	0.181(6)	0.161(3)	0.1672(9)	0.2990(8)
1.90	0.1401(6)	0.1171(2)	0.1232(4)	0.291(5)
3	0.077(2)	0.058(2)		

We have recently shown in Figure 16 of Ref. [87] that the product of the diffusion coefficient of water times the viscosity of the solution seems to be constant, not depending on either the concentration of the salt or the type of salt (i.e. the water molecules satisfy a Stokes-Einstein-like relation even in solution). If this is the case, it means that the increase in the diffusion coefficient of water in the K_2SO_4 solutions implies a decrease in the viscosity of the solution. The surprising finding is that the same salt can increase the viscosity relative to water at room temperature and decrease the viscosity relative to water at 240 K. Thus, temperature significantly influences the changes provoked by the electrolyte in water.

Although we do not necessarily share this view, some authors refer to electrolytes that increase the viscosity of water as 'structure makers' and those that decrease the viscosity of water as 'structure breakers' (typically expressed by the sign of the parameter B in the Dole equation). In this context, K_2SO_4 is a structure maker at room temperature and a structure breaker at low temperatures.

From a kinetic perspective, Mg, Li, and Na are more structure makers than K. However, when looking at the results in Table 4, it appears that K is the ion that perturbs the structure of water the least, as it presents the most negative value of the water-water potential energy. These concepts seem rather diffuse, and here we focus on the facts (i.e. potential energies, diffusion coefficients, viscosities) and refrain from translating these numbers into simple terms or pictures. We leave the interpretation of the facts to the reader. The key point is that at low temperatures, the increase in the viscosity of water due to the presence of salt is significantly reduced, and in some cases, such as with K_2SO_4, the presence of salt can even cause a decrease in the viscosity of the system.

3. Conclusions

In this work we have studied by means of molecular dynamics four sulfate water mixtures, Li_2SO_4, $MgSO_4$, Na_2SO_4 and K_2SO_4. The simulations have taken place at different concentrations at ambient temperature and upon supercooling, 240 K, at ambient pressure. The RDFs of water oxygens, $g_{O_wO_w}(r)$, displayed increased perturbations with higher salt concentrations, particularly pronounced at the lower temperature of 240 K.

For Li_2SO_4, Na_2SO_4, and K_2SO_4 solutions up to 1.30 mol kg^{-1}, the decreased height of the first peak and shallower first minimum indicate a reduced order in the water structure. This effect mirrors the structural changes observed under high pressure in pure water, suggesting an increase in distorted tetrahedra [39].

At 1.90 mol kg^{-1}, K_2SO_4 showed an anomaly, with a less significant impact on the water structure at ambient temperature, but at 240 K, higher peaks and deeper minima suggested a more ordered water structure.

For $MgSO_4$, there was an increase in the first peak height without notable enhancement at lower temperatures. However, the first minimum filled in at 240 K, and a new second peak emerged around 0.38 nm, indicating significant structural perturbation likely due to magnesium ions displacing water molecules in the coordination layer.

All salts showed higher first peaks in the RDFs at lower temperatures, indicating more ordered structures. Notably, Na_2SO_4 was a strong structure breaker, significantly reducing the height of the first peak and depth of the first minimum compared to other salts. In contrast, $MgSO_4$ exhibited the opposite effect.

The analysis of the orientational order parameter q_t corroborated the RDF findings, indicating a general loss of tetrahedrality in the water structure. Besides Li_2SO_4 and $MgSO_4$ displayed additional peaks, with $MgSO_4$ causing the most significant structural changes.

Examining hydrogen bond networks through $g_{O_wH}(r)$ and $g_{HH}(r)$ showed less perturbation than the oxygen structure but still notable effects at lower temperatures. K_2SO_4 at 1.90 mol kg^{-1} again showed anomalous behaviour, indicating different effects on water structure at varying concentrations and temperatures.

Finally, diffusion coefficients revealed that salt concentration generally reduced water diffusion at 300 K, with K_2SO_4 having the mildest effect. At 240 K, diffusion coefficients for Li, Na, and Mg sulfates decreased less with concentration, while K_2SO_4 showed an unexpected increase, suggesting a decrease in solution viscosity at lower temperatures.

In summary, sulfate salts impact water structure significantly, with $MgSO_4$ causing the largest perturbation. The behaviour varies with temperature and concentration, highlighting the complex interactions between ions and water molecules. These findings advance our

understanding of electrolyte solutions and their influence on water structure and dynamics.

Acknowledgments

We would like to dedicate this paper to the memory of Prof. Luis Rull who played a key role in the development of Statistical Mechanics in Spain and formed a number of young students that developed their careers all around the world. And we would like to extend our deepest gratitude to our colleague and friend José Luis Fernández Abascal for his outstanding contributions to the field of computer simulations specially of water. His groundbreaking research and unwavering dedication have significantly advanced our understanding. We are honoured to dedicate this work to J. L. F. Abascal, in recognition of his remarkable achievements.

Disclosure statement

No potential conflict of interest was reported by the author(s).

Funding

C.P.L and C.V would like to thank the funding grant number PID2022-136919NB-C31 of the Ministerio de Ciencia, Innovación y Universidades. C. P. L. thanks Ministerio de Ciencia, Innovación y Universidades for a predoctoral Formación Profesorado Universitario grant number FPU18/03326 and the research stay grant number EST21/00256.

ORCID

Cintia P. Lamas http://orcid.org/0000-0001-9453-1205
Carlos Vega http://orcid.org/0000-0002-2417-9645
Paola Gallo https://orcid.org/0000-0003-4370-9071

References

[1] P. Jungwirth and D.J. Tobias, Chem. Rev. **106** (4), 1259–1281 (2006). doi:10.1021/cr0403741
[2] P.G. Debenedetti, J. Phys. Cond. Mat. **15** (45), R1669 (2003). doi:10.1088/0953-8984/15/45/R01
[3] P. Gallo, K. Amann-Winkel, C.A. Angell, M.A. Anisimov, F. Caupin, C. Chakravarty, E. Lascaris, T. Loerting, A.Z. Panagiotopoulos, J. Russo, J.A. Sellberg, H.E. Stanley, H. Tanaka, C. Vega, L. Xu and L.G.M. Pettersson, Chem. Rev. **116** (13), 7463–7500 (2016). doi:10.1021/acs.chemrev.5b00750
[4] P. Gallo and H.E. Stanley, Science **358** (6370), 1543–1544 (2017). doi:10.1126/science.aar3575
[5] P.H. Poole, F. Sciortino, U. Essmann and H.E. Stanley, Nature **360** (6402), 324–328 (1992). doi:10.1038/360324a0
[6] R. Mancinelli, A. Botti, F. Bruni, M. Ricci and A. K. Soper, J. Phys. Chem. B **111** (48), 13570–13577 (2007). doi:10.1021/jp075913v
[7] J.E. Enderby, Chem. Soc. Rev. **24** (3), 159–168 (1995). doi:10.1039/cs9952400159
[8] G. Herdman and G. Neilson, J. Mol. Liq. **46**, 165–179 (1990). doi:10.1016/0167-7322(90)80052-L
[9] H. Ohtaki and T. Radnai, Chem. Rev. **93** (3), 1157–1204 (1993). doi:10.1021/cr00019a014
[10] A. K. Soper, J. Chem. Phys. **101** (8), 6888–6901 (1994). doi:10.1063/1.468318
[11] A.K. Soper and M.A. Ricci, Phys. Rev. Lett. **84** (13), 2881 (2000). doi:10.1103/PhysRevLett.84.2881
[12] G. Neilson, P. Mason, S. Ramos and D. Sullivan, Philos. Trans. A Math. Phys. Eng. Sci. **359** (1785), 1575–1591 (2001). doi:10.1098/rsta.2001.0866
[13] Y. Lü and B. Wei, J. Chem. Phys. **125** (14), 144503 (2006). doi:10.1063/1.2358134
[14] R. Mancinelli, A. Botti, F. Bruni, M. Ricci and A. K. Soper, Phys. Chem. Chem. Phys. **9** (23), 2959–2967 (2007). doi:10.1039/b701855j
[15] M. Galib, M.D. Baer, L.B. Skinner, C.J. Mundy, G.K. Schenter, T. Huthwelker, C.J. Benmore, J. Pham, N. Govind and J.L. Fulton, J. Chem. Phys. **146** (8), 084504 (2017). doi:10.1063/1.4975608
[16] H. Shinto, T. Sakakibara and K. Higashitani, J. Phys. Chem. B **102**, 1974 (1998). doi:10.1021/jp972795a
[17] K. Kobayashi, Y. Liang, T. Sakka and T. Matsuoka, J. Chem. Phys. **140** (14), 144705 (2014). doi:10.1063/1.4870417
[18] L. Vrbka and P. Jungwirth, Phys. Rev. Lett. **95** (14), 148501 (2005). doi:10.1103/PhysRevLett.95.148501
[19] D. Corradini, P. Gallo and M. Rovere, J. Condens. Matter Phys. **22**, 284104 (2010). doi:10.1088/0953-8984/22/28/284104
[20] D. Corradini, M. Rovere and P. Gallo, J. Chem. Phys. **132** (13), 134508 (2010). doi:10.1063/1.3376776
[21] D. Corradini and P. Gallo, J. Phys. Chem. B **115** (48), 14161–14166 (2011). doi:10.1021/jp2045977
[22] J.L. Aragones, M. Rovere, C. Vega and P. Gallo, J. Phys. Chem. B **118** (28), 7680–7691 (2014). doi:10.1021/jp500937h
[23] M.M. Conde, M. Rovere and P. Gallo, Phys. Chem. Chem. Phys. **19**, 9566–9574 (2017). doi:10.1039/C7CP00665A
[24] M.M. Conde, M. Rovere and P. Gallo, Phys. Chem. Chem. Phys. **19** (14), 9566–9574 (2017). doi:10.1039/C7CP00665A
[25] M.M. Conde, M. Rovere and P. Gallo, J. Molec. Liq. **261**, 513–519 (2018). doi:10.1016/j.molliq.2018.03.126
[26] C.P. Lamas, C. Vega and E.G. Noya, J. Chem. Phys. **156** (13), 134503 (2022). doi:10.1063/5.0085051
[27] V. Bianco, M. Conde, C. Lamas, E.G. Noya and E. Sanz, J. Chem. Phys. **156** (6), 064505 (2022). doi:10.1063/5.0083371
[28] S. Bauerecker, P. Ulbig, V. Buch, L. Vrbka and P. Jungwirth, J. Phys. Chem. C **112** (20), 7631–7636 (2008). doi:10.1021/jp711507f
[29] G.D. Soria, J.R. Espinosa, J. Ramirez, C. Valeriani, C. Vega and E. Sanz, J. Chem. Phys. **148** (22), 222811 (2018). doi:10.1063/1.5008889
[30] J.R. Espinosa, G.D. Soria, J. Ramirez, C. Valeriani, C. Vega and E. Sanz, J. Phys. Chem. Lett. **8**, 4486 (2017). doi:10.1021/acs.jpclett.7b01551
[31] D. Chakraborty and G. Patey, Chem. Phys. Lett. **587**, 25–29 (2013). doi:10.1016/j.cplett.2013.09.054
[32] D. Chakraborty and G.N. Patey, J. Phys. Chem. Lett. **4** (4), 573–578 (2013). doi:10.1021/jz302065w

[33] H. Jiang, A. Haji-Akbari, P.G. Debenedetti and A. Panagiotopoulos, J. Chem. Phys. **148** (4), 044505 (2018). doi:10.1063/1.5016554

[34] C.P. Lamas, J.R. Espinosa, M.M. Conde, J. Ramírez, P.M. de Hijes, E.G. Noya, C. Vega and E. Sanz, Phys. Chem. Chem. Phys. **23** (47), 26843–26852 (2021). doi:10.1039/D1CP02093E

[35] D. Corradini, M. Rovere and P. Gallo, J. Phys. Chem. B **115** (6), 1461–1468 (2011). doi:10.1021/jp1101237

[36] P. Gallo, D. Corradini and M. Rovere, J. Chem. Phys. **139** (20), 204503 (2013). doi:10.1063/1.4832382

[37] G. Cassinello, E. G. Noya, E. Sanz, and C. P. Lamas, Mol. Phys. e2398133 (2024). doi:10.1080/00268976.2024.2398133

[38] S. Zhang, D. Tan, H. Zhu, H. Pei and B. Shi, J. Rock Mech. Geotech. Eng. (2024).

[39] J. Holzmann, R. Ludwig, A. Geiger and D. Paschek, Angew. Chem. Int. Ed. **46** (46), 8907–8911 (2007). doi:10.1002/anie.v46:46

[40] P. Gallo, D. Corradini and M. Rovere, J. Mol. Liq. **189**, 52–56 (2014). doi:10.1016/j.molliq.2013.05.023

[41] L. Perin and P. Gallo, J. Phys. Chem. B **127** (20), 4613–4622 (2023). doi:10.1021/acs.jpcb.3c00703

[42] P. Gallo, M. Martin Conde, D. Corradini, P. Pugliese and M. Rovere, *Structural Properties of Ionic Aqueous Solutions* (Springer International Publishing, Cham, 2018), pp. 153–162.

[43] P. Gallo, D. Corradini and M. Rovere, Phys. Chem. Chem. Phys. **13** (44), 19814–19822 (2011). doi:10.1039/c1cp22166c

[44] R. Nakamura, S. Machida, Y. Ogata and T. Ogawa, J. Phys. Chem. B **120** (28), 7281–7290 (2016).

[45] T.-M. Chang and L.X. Dang, J. Phys. Chem. B **113** (4), 1213–1221 (2009).

[46] S. Roy, A. Hossain, K. Mahali and B. Dolui, Russ. J. Phys. Chem. A **89**, 2111–2119 (2015). doi:10.1134/S0036024415110151

[47] B. Ghosh, S. Chowdhury, N. Sing, P. Mondal, M. Mondal, B.C. Hansda, S. Roy, A. Henaish, J. Ahmed and K. Mahali, J. Mol. Liq. **385**, 122432 (2023). doi:10.1016/j.molliq.2023.122432

[48] M.O. Andreae, C.D. Jones and P.M. Cox, Nature **435** (7046), 1187–1190 (2005). doi:10.1038/nature03671

[49] R.J. Charlson, S. Schwartz, J. Hales, R.D. Cess, J. Coakley Jr, J. Hansen and D. Hofmann, Science**255** (5043), 423–430 (1992). doi:10.1126/science.255.5043.423

[50] W.L. Jorgensen, J. Chandrasekhar, J.D. Madura, R.W. Impey and M.L. Klein, J. Chem. Phys. **79**, 926–935 (1983). doi:10.1063/1.445869

[51] H.J.C. Berendsen, J.R. Grigera and T.P. Straatsma, J. Phys. Chem. **91** (24), 6269–6271 (1987). doi:10.1021/j100308a038

[52] M.W. Mahoney and W.L. Jorgensen, J. Chem. Phys. **112**, 8910–8922 (2000). doi:10.1063/1.481505

[53] H.W. Horn, W.C. Swope, J.W. Pitera, J.D. Madura, T.J. Dick, G.L. Hura and T. Head-Gordon, J. Chem. Phys. **120**, 9665 (2004). doi:10.1063/1.1683075

[54] J.L.F. Abascal and C. Vega, J. Chem. Phys. **123** (23), 234505 (2005). doi:10.1063/1.2121687

[55] I.M. Zeron, J.L.F. Abascal and C. Vega, J. Chem. Phys. **151** (13), 134504 (2019). doi:10.1063/1.5121392

[56] I.M. Zeron, M.A. Gonzalez, E. Errani, C. Vega and J.L.F. Abascal, J. Chem. Theory Comput. **17**, 1715 (2021). doi:10.1021/acs.jctc.1c00072

[57] I.V. Leontyev and A.A. Stuchebrukhov, J. Chem. Phys. **130**, 085102 (2009). doi:10.1063/1.3060164

[58] I.V. Leontyev and A.A. Stuchebrukhov, J. Chem. Theory Comput. **6** (10), 3153–3161 (2010). doi:10.1021/ct1002048

[59] I.V. Leontyev and A.A. Stuchebrukhov, Phys. Chem. Chem. Phys. **13**, 2613–2626 (2011). doi:10.1039/c0cp01971b

[60] C. Vega, Mol. Phys. **113**, 1145 (2015). doi:10.1080/00268976.2015.1005191

[61] M. Kohagen, P.E. Mason and P. Jungwirth, J. Phys. Chem. B **118** (28), 7902–7909 (2014). doi:10.1021/jp5005693

[62] T. Martinek, E. Duboué-Dijon, V. Timr, P.E. Mason, K. Baxová, H.E. Fischer, B. Schmidt, E. Pluhařová and P. Jungwirth, J. Chem. Phys. **148** (22), 222813 (2018). doi:10.1063/1.5006779

[63] E. Duboué-Dijon, P.E. Mason, H.E. Fischer and P. Jungwirth, J. Phys. Chem. B **122** (13), 3296–3306 (2017). doi:10.1021/acs.jpcb.7b09612

[64] M. Kohagen, P.E. Mason and P. Jungwirth, J. Phys. Chem. B **120** (8), 1454–1460 (2015). doi:10.1021/acs.jpcb.5b05221

[65] E. Pluhařová, P.E. Mason and P. Jungwirth, J. Phys. Chem. A **117** (46), 11766–11773 (2013). doi:10.1021/jp402532e

[66] Z. Kann and J. Skinner, J. Chem. Phys. **141** (10), 104507 (2014). doi:10.1063/1.4894500

[67] R. Fuentes-Azcatl and M.C. Barbosa, J. Phys. Chem. B **120** (9), 2460–2470 (2016). doi:10.1021/acs.jpcb.5b12584

[68] M. Predota and D. Biriukov, J. Mol. Liq. **314**, 113571 (2020). doi:10.1016/j.molliq.2020.113571

[69] S. Blazquez, M. Conde and C. Vega, J. Chem. Phys. **158** (5), 054505 (2023). doi:10.1063/5.0136498

[70] L. F. Sedano, S. Blazquez, E.G. Noya, C. Vega and J. Troncoso, J. Chem. Phys. **156** (15), 154502 (2022). doi:10.1063/5.0087679

[71] F. Gámez, L. F. Sedano, S. Blázquez, J. Troncoso and C. Vega, J. Mol. Liq. **377**, 121433 (2023). doi:10.1016/j.molliq.2023.121433

[72] E. Bock, Can. J. Chem. **39** (9), 1746–1751 (1961). doi:10.1139/v61-228

[73] S. Pengsheng and Y. Yan, Calphad **27** (4), 343–352 (2003). doi:10.1016/j.calphad.2004.02.001

[74] B. Hess, C. Kutzner, D. Van Der Spoel and E. Lindahl, J. Chem. Theory Comput. **4** (3), 435–447 (2008). doi:10.1021/ct700301q

[75] M. Parrinello and A. Rahman, J. Appl. Phys. **52** (12), 7182–7190 (1981). doi:10.1063/1.328693

[76] G.J. Martyna, M.L. Klein and M. Tuckerman, J. Chem. Phys. **97** (4), 2635–2643 (1992). doi:10.1063/1.463940

[77] D.R. Wheeler and J. Newman, Chem. Phys. Lett. **366** (5-6), 537–543 (2002). doi:10.1016/S0009-2614(02)01644-5

[78] J.-P. Ryckaert, G. Ciccotti and H.J.C. Berendsen, J. Comput. Phys. **23** (3), 327–341 (1977). doi:10.1016/0021-9991(77)90098-5

[79] M. Laliberte and W.E. Cooper, J. Chem. Eng. Data **49** (5), 1141–1151 (2004). doi:10.1021/je0498659
[80] M. Laliberte, J. Chem. Eng. Data **54** (6), 1725–1760 (2009). doi:10.1021/je8008123
[81] S. Mao, Q. Peng, M. Wang, J. Hu, C. Peng and J. Zhang, Appl. Geochem. **86**, 105–120 (2017). doi:10.1016/j.apgeochem.2017.10.002
[82] Y. Marcus, *Ion Properties*, Vol. 1 (CRC Press, 1997).
[83] J.R. Errington and P.G. Debenedetti, Nature **409** (6818), 318–321 (2001). doi:10.1038/35053024
[84] J.S. Kim and A. Yethiraj, J. Phys. Chem. B **112** (6), 1729–1735 (2008). doi:10.1021/jp076710+
[85] F.W. Starr, S. Harrington, F. Sciortino and H.E. Stanley, Phys. Rev. Lett. **82** (18), 3629 (1999). doi:10.1103/PhysRevLett.82.3629
[86] L. Lupi and P. Gallo, J. Chem. Phys. **159** (15), 154504 (2023). doi:10.1063/5.0168933
[87] S. Blazquez, M.M. Conde, J. L. F. Abascal and C. Vega, J. Chem. Phys. **156** (4), 044505 (2022). doi:10.1063/5.0077716